A Global View of 3D Cloud Structure from a Decade of Space-borne Radar Measurements

Thumree Sarkar,

Centre for Atmospheric Sciences, Indian Institute of Technology Delhi, Hauz Khas, New Delhi, India
thumrees1988@gmail.com

Sagnik Dey

Centre for Atmospheric Sciences, Indian Institute of Technology Delhi, Hauz Khas, New Delhi, India
sagnikdey.iitd@gmail.com

Dilip Ganguly

Centre for Atmospheric Sciences, Indian Institute of Technology Delhi, Hauz Khas, New Delhi, India
ganguly.dilip@gmail.com

***Abstract*— Clouds influence the planet's energy and hydrological balance. Poorly resolved clouds in climate models produce an unacceptable discrepancy in the global heat and moisture transport. Robust studies quantifying the cloud in a 3-D observational framework is critical to resolve the aerosol-cloud-precipitation cycle and active remote sensing can prove to be very useful for this purpose. Here, we present the three dimensional global cloud climatology of individual cloud types using satellite based active radar measurement. We find that global mean cloud fractions of cumulus, stratocumulus-stratus (combined), altocumulus, altostratus, nimbostratus, cirrus and deep convective clouds from Cloudsat are 4.7%, 15.9% , 6.1%, 7.1%, 4.1%, 5.7% and 1.4% respectively. The work is expected to generate key strategic knowledge about characteristics of precipitating and non-precipitating clouds which will be useful to the modeling community trying to improve the climate models in the Indian monsoon region.**

Keywords—Cloud types, CloudSat, Remote sensing, JJA season

I. INTRODUCTION

The ever-changing structure and constituent of clouds influence the formation and evolution of the Earth's storm structures as well as regulates the long and shortwave propagation through atmosphere. In this way clouds govern the hydrological and energy budget of earth [1]. Even a slight variation in the amount or location of clouds can modify the climate more than the estimated changes by anthropogenic emissions, greenhouse gases and other aspects associated with climate change. Moreover, different cloud types namely cumulus (CU), stratocumulus (SC), stratus (ST), altostratus (AS), altocumulus (AC), nimbostratus (NS), cirrus (CI) and deep convective (DC) clouds have different radiative and microphysical properties [2]. Lack of understanding of these properties related to cloud dynamics [3] contributes the largest uncertainty in climate forcing in models [4]. Utilisation of various observational datasets from various satellites and in-situ data sources can be seen as the way forward to quantify the cloud morphology and identify the gaps in the climate models.

The Global Energy and water Cycle Experiment (GEWEX) Radiation Panel initiated a cloud assessment programme in 2005 to compare the long term available cloud data products. They characterized the cloud properties and their variations for visualising the cloud dynamical processes and radiative effects. GEWEX programme includes ISCC, MISR, ATSR-GRAPE, POLDER, MODIS, HIRS NOAA, TOVS, PATMOSx and one active measurement source CALIPSO. While such efforts have provided new knowledge, the interpretation from passive sensors is biased towards single layer clouds and cannot confidently discriminate between some key cloud and precipitation states. They are not sensitive enough to resolve the altitudinal variation of cloud systems let alone the multi-layer cloud. Though CALIPSO uses active remote sensing technology, but the lidar is highly sensitive towards detecting sub-visible cirrus clouds, its beam can only reach cloud base with an optical depth less than 3.

Active remote sensing data from CLOUDSAT can be very useful for this purpose. It is a 705 km altitude sun-synchronous polar-orbiting satellite, was launched in April 2006, as part of the A-Train constellation of satellites [5]. The CPR on the CloudSat is a 94 GHz (3 mm), nadir-viewing radar. Recent CloudSat radar observations represent an extraordinary and exclusive prospect to address the multi-layer clouds at regional and global scales. There are studies on cloud distribution and dynamics by many groups [6, 7, 8]. However, the cloud type distribution over whole globe in a multi-layered cloud system in long term basis is still not there. Thus the purpose of this paper is to analyze 3-D cloud climatology of different cloud types and reviewing the seasonal and altitudinal dependence over the globe using a decade (2007–2016) of CloudSat data products.

II. METHODOLOGY

Ten years (2007-2016) of CloudSat observations during the northern-hemispherical summer monsoon months (June-July-August: JJA), over the globe region is taken into account for the present study. CloudSat provides high resolution vertical cloud profiles across the globe and has a return period of approximately 16 days [9]. The CPR on-board has a minimum detectable reflectivity of approximately 30 dBZ, a 70-dBZ dynamic range, and a calibration accuracy of 1.5 dBZ. The footprint spatial resolution is 2.6×1.4 km and the effective vertical resolution at nadir is 240 m. CPR is not sensitive to optically thin clouds such as high-altitude cirrus clouds and it cannot function well below 5 km altitude due to errors introduced by ground clutter [10]. The 2B Geoprof and 2B-CLDCLASS data products are used for the present study. Details about 2B Geoprof data product can be found in [11] and [12]. For the present study, the observations over the study region are grouped into 2.5×2.5 grid boxes keeping the vertical resolution same as the CPR. The CF (in %) for individual cloud type is calculated using cloud amount calculation

method described in [13] using the cloud classification data of 2B CLDCLASS data product. SC and ST clouds are combined together and presented as SS cloud type for the whole study.

III. Results and Discussion

A. Global Distribution of Cloud Fraction

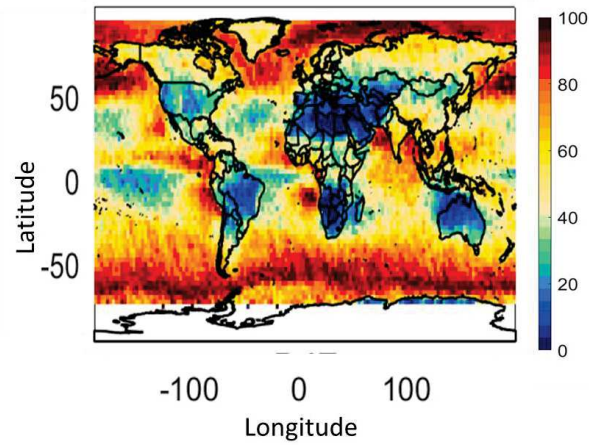

Fig. 1 Total Cloud Fraction (CF in %) for JJA season.

Seasonal mean CF (CF_{Tot}) of total detectable cloud is shown in Fig.1. CF_{Tot} in the Inter-Tropical Convergence Zone (ITCZ), southern ocean and Arctic Ocean region is found to be high (CF_{Tot} >80) in JJA. The arid African Sahara and Kalahari Desert remain cloud free (CF_{Tot} <10) most of the time in the year. In JJA the ITCZ is found to lie north of the equator. The high CF_{Tot} can be associated with the world's strongest monsoons stretching in Asia, some parts of Africa, America and northern Australia. South Asian countries such as Vietnam, Thailand, Cambodia, Bangladesh, Laos, India, and Pakistan encounter heavy rainfall in JJA. Over Africa the ITCZ lies just south of the Sahara Desert (Sub-Saharan Africa) and countries such as Mali, Niger, Ghana, and the Ivory Coast experience summer monsoon. CF varies with the seasons in the tropical parts of North America, Central America, and South America, even in areas where rainforests thrive. Costa Rica, Nicaragua, Panama, and western Mexico, these parts also remain associated with high CF_{Tot} and rain in JJA.

B. Relative Contribution of Multilayered Cloud

The global maps of multi-layered clouds provide much needed quantification of vertically resolved clouds. From Fig. 2 it can be observed that there is an ubiquitous presence of multi-layered cloud all over globe. The multi-layered cloud fraction (CF_{Multi}) is seen to be very less dependent on CF_{Tot}. Global ocean has high CF_{Multi} than land surface. It is evident from the Fig.2 that ITCZ, southern ocean and Arctic Ocean, where CF_{Tot} is high (CF_{Tot}>80). Some southern parts of Africa near Namibian desert and Brazilian highland the CF_{Multi} is less than 20. North America and Canada also have CF_{Multi} less than 70 for all other land regions in these seasons CF_{Multi} is greater than 70.

This extensive presence of multi-layered cloud thus demands segregation of clouds further to observe their structural distribution in three dimensions.

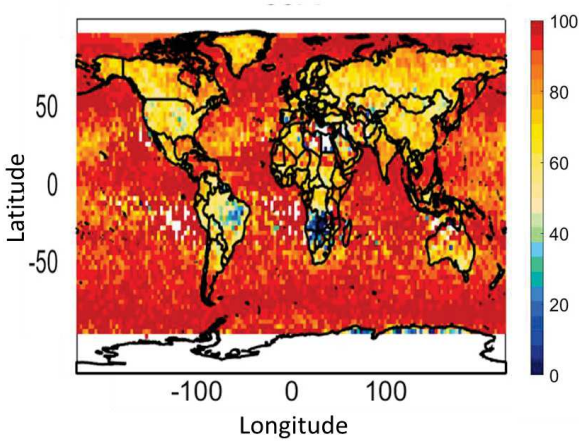

Fig. 2 Cloud occurrence frequency of Multi-layered cloud in JJA season.

C. Seasonal three-dimensional cloud climatology

The 3-D distributions of different cloud types show the rich morphology detectable from space. The combined spatial and vertical distribution of each individual cloud types gives the 3-D distribution of monsoon clouds over globe.

a) Spatial Cloud cover over globe

The spatial distributions of different cloud types show the selective presence of different cloud at different regions of the globe and their seasonal dependence. In the present section, the discussion is done for each cloud type and their distribution for each season. Altocumulus (AC) clouds are mid altitude clouds. The Cloud fraction of AC clouds (CF_{AC}) is higher in northern land surface for Northern Summer Monsoon season (JJA). CF_{AC} is high in northern hemisphere in JJA season. High CF of AC in Asia and India can be directly connected to the Asian summer monsoon. Southern hemispherical land masses has very low CF_{AC} (CF_{AC} <2) in JJA season.

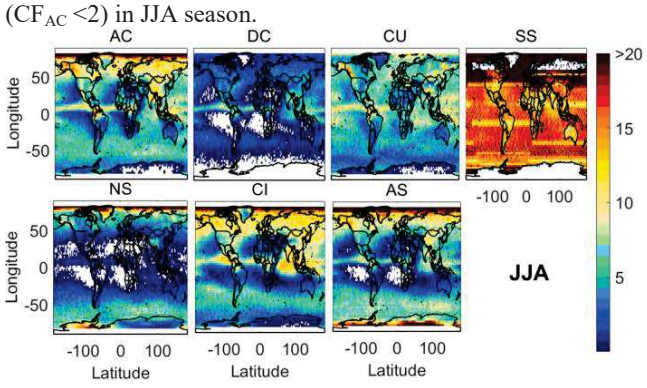

Fig. 3 Spatial distribution of (a) CF_{AC}, (b) CF_{DC}, (c) CF_{CU}, (d) CF_{SS} (SC+ST), (e) CF_{NS}, (f) CF_{CI} and (g) CF_{AS} in % averaged over the globe during 2007–2016 JJA season.

Deep convective (DC) clouds are tropical clouds which has lower mean surface cloud fraction (CF_{DC}) than most of the cloud types. However, this cloud is the most effective one in governing the hydrological cycle in terms of causing heavy rainfall in ITCZ region. In JJA there is a significant amount

of DC clouds present in Bay of Bengal in the east coast of India and Indo-China peninsula. On the other hand, in the west coasts of Africa and South-America CF_{DC} is very low in JJA. CloudSat CPR is not much sensitive in retrieving information for very low clouds for the error associated with ground clutter. Thus the spatial distribution of SC and ST cloud (combined as SS) is not very clear from the Fig. 3.

CU clouds are also low level clouds but their vertical stretch is more than SC and ST clouds. Thus CloudSat retrieval is better for CU clouds. CU cloud fraction (CF_{cu}) over land regions varies significantly with the seasonal changes. For JJA season CF_{cu} is high (CF_{cu}>10) for ITCZ, Tibetan platue and northern arctic. In India, Indo-China Peninsula, Canadian Rocky and southern Russia a significant increase in the CF_{cu} (CF_{cu} >12) can be observed from the Fig 3 (CU). NS clouds are mostly found stretched from mid-latitude to pole wards on both hemispheres. The NS cloud fraction (CF_{NS}) is not much dependent on the seasonal variations. In the tropical belt, only Tibetan plateau is seen to have NS clouds with an average value of CF_{NS} (CF_{NS} ~6) in JJA. Retrieved cloud fraction of CI cloud (CF_{CI}), the high and thin ice clouds is less than the actual amount of CI cloud present in the atmosphere due to less sensitivity of CloudSat CPR. JJA season is associated with very high CF_{CI} in Northern hemisphere. In the Arabian Sea, Bay of Bengal and northern part of Indian ocean can be seen to have high CF_{CI} (CF_{CI} >12). There is very less CF_{CI} (CF_{CI} < 2) in Europe and Northern part of Africa. AS cloud is mostly stretched from midlatitude storm tracks to the polar latitudes like NS clouds. Only difference comes with the presence of AS clouds in ITCZ. In JJA for Indian summer monsoon region high fraction of CF_{AS} is present (CF_{AS} >10).

Table 1: Global mean cloud fraction from CloudSat

Cloud Types	CU	SS	AS	AC	NS	CI	DC
JJA	4.8	16.1	6.9	6.8	3.5	6.7	1.8

b) Altitudinal variation of cloud fraction

The zonal mean of different cloud types are shown in Fig. 4 to have a detailed understanding of the altitudinal variation of the seven cloud types. The altitudinal selection of different clouds at different latitudes shows the complexity of possible combinations in the multi-layered cloud systems. In JJA the CF_{AC} remains (>8) near equator and there is a significant high value (>12) in northern storm tracks. The primary alterations of CF_{AC} is concentrated in 2-5 km altitude range, below or above this range CF_{AC} is insignificant (CF_{AC} <1) except for the equator (CF_{AC}~5). The altitudinal stretch of CF_{DC} is highest (0-15 km in the equator) and the latitudinal stretch is lowest (maximum -30^0 to $+30^0$) for DC clouds. The highest CF_{DC} (CF_{DC}~4) is present near equator which has a slight spread towards mid-latitudes in MAM and SON. A longer stretch towards northern and southern latitude with increase in CF can be observed in JJA and DJF respectively. The CU cloud also follows the latitudinal selection of DC clouds with a stretch in latitudes up to -30^0 to $+30^0$. CF_{CU} is highest for equator ~6 and for the stretch towards higher latitudes, CF_{CU} is ~4 except for JJA. In case of JJA there is an increase in CF_{DC} around $+30^0$ latitude (~6). The altitudinal stretch of CF_{CU} having values >2 is from 0-5 km which is much less than DC clouds.

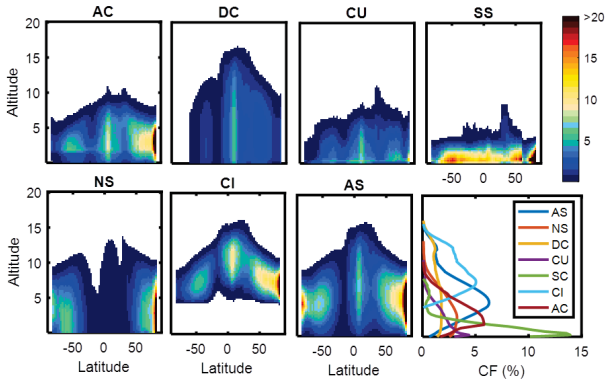

Fig. 4 Zonal mean of (a) CF_{AC}, (b) CF_{DC}, (c) CF_{CU}, (d) CF_{SS} (SC+ST), (e) CF_{NS}, (f) CF_{CI} and (g) CF_{AS} in % averaged over the globe during 2007–2016 JJA season.

High CF_{SS} (CF_{SS} >12) is observed uniformly stretched with an increase in the northern polar regions with values CF_{SS}>18. The variation of these clouds is very less dependent on seasonal changes. The altitudinal stretch with CF_{SS}>2 is 0-2 km. NS clouds are stretched form mid-latitude storm tracks to polar regions, as already discussed in the previous section. The altitudinal stretch is for NS (CF_{NS} >2) is 0-8 kms from mid-latitude to polar region. CI, the high clouds has the cloud bottom layer around 7 km and top around 15 km in tropics and the stretch is 5-10 km for other latitudes when CF_{CI}>2 . Maximum CF_{CI} (CF_{CI}>12) is observed in equatorial region with some stretch toward mid-latitudes in JJA season. AS cloud have similarity in their latitudinal selection as the AC clouds, however the CF_{AS} is much higher in polar regions than in equator and the cloud base and top are also higher than AC. The CF_{AS} (CF_{AS} >2) is stretched 2-15 kms in equator and 1-10 in polar region.

IV. Conclusions

The study provides the long term three dimensional cloud climatology of individual cloud types for the first time. Quantification of 3-D cloud cover in Northern-hemispherical summer monsoon region will be very useful for modelling community for validation purpose. The extension of this work comprising detailed analysis of clouds in different seasons will further enrich the understanding of the structure of multi-layered cloud systems.

Acknowledgment

The work is carried out under the National Post-Doctoral Fellowship (PDF/2017/000119) of Science and Engineering Research Board (SERB), Govt. of India.

References

[1] Stephens, G. L. (2005). Cloud feedbacks in the climate system: A critical review. Journal of Climate, 18(2), 237-273.

[2] Chen, T., Rossow, W. B., & Zhang, Y. (2000). Radiative effects of cloud-type variations. Journal of Climate, 13(1), 264-286.

[3] Wielicki, B. A., Wong, T., Allan, R. P., Slingo, A., Kiehl, J. T., Soden, B. J., ... & Robertson, F. (2002). Evidence for large decadal variability in the tropical mean radiative energy budget. Science, 295(5556), 841-844.

[4] Boucher, O., Randall, D., Artaxo, P., Bretherton, C., Feingold, G., Forster, P., ... & Rasch, P. (2013). Clouds and aerosols. In Climate change 2013: the physical science basis. Contribution of Working Group I to the Fifth Assessment Report of the Intergovernmental Panel on Climate Change (pp. 571-657). Cambridge University Press.

[5] Stephens, G. L., Vane, D. G., Tanelli, S., Im, E., Durden, S., Rokey, M., ... & L'Ecuyer, T. (2008). CloudSat mission: Performance and early science after the first year of operation. Journal of Geophysical Research: Atmospheres, 113(D8).

[6] Sassen, K., & Wang, Z. (2008). Classifying clouds around the globe with the CloudSat radar: 1 - year of results. Geophysical Research Letters, 35(4).

[7] Subrahmanyam, K. V., & Kumar, K. K. (2017). CloudSat observations of multi layered clouds across the globe. Climate Dynamics, 49(1-2), 327-341.

[8] Rajeevan, M., Rohini, P., Kumar, K. N., Srinivasan, J., & Unnikrishnan, C. K. (2013). A study of vertical cloud structure of the Indian summer monsoon using CloudSat data. Climate Dynamics, 40(3-4), 637-650.

[9] Stephens, G. L., Vane, D. G., Boain, R. J., Mace, G. G., Sassen, K., Wang, Z., ... & Miller, S. D. (2002). The CloudSat mission and the A-Train: A new dimension of space-based observations of clouds and precipitation. Bulletin of the American Meteorological Society, 83(12), 1771-1790.

[10] Behrangi, A., Kubar, T., & Lambrigtsen, B. (2012). Phenomenological description of tropical clouds using CloudSat cloud classification. Monthly Weather Review, 140(10), 3235-3249.

[11] Mace, G. G., Marchand, R., Zhang, Q., & Stephens, G. (2007). Global hydrometeor occurrence as observed by CloudSat: Initial observations from summer 2006. Geophysical Research Letters, 34(9).

[12] Marchand, R., Mace, G. G., Ackerman, T., & Stephens, G. (2008). Hydrometeor detection using CloudSat—An Earth-orbiting 94-GHz cloud radar. Journal of Atmospheric and Oceanic Technology, 25(4), 519-533.

[13] Stubenrauch, C. J., Rossow, W. B., Kinne, S., Ackerman, S., Cesana, G., Chepfer, H., ... & Maddux, B. C. (2013). Assessment of global cloud datasets from satellites: Project and database initiated by the GEWEX radiation panel. Bulletin of the American Meteorological Society, 94(7), 1031-1049.